Rapid report

Involvement of a novel fast inward sodium current in the invasion capacity of a breast cancer cell line

Sébastien Roger, Pierre Besson, Jean-Yves Le Guennec*

Nutrition, Croissance et Cancer, Inserm Emi-U 0211, Faculté de Médecine, 2 Bd Tonnellé, 37032 Tours Cedex, France

Abstract

This work reports the finding of a unique fast inward sodium current (I_{Na}) in MDA-MB-231 cells which is missing in MDA-MB-468 cells and in MCF-7 cells. This current is high-voltage-activated and displays a window current at the membrane potential of MDA-MB-231 cells. This current is blocked by high concentrations of tetrodotoxin (TTX). In MDA-MB-231 cells, which are the most invasive cells among the three cell lines tested, proliferation and migration were not sensitive to TTX while invasion was reduced by approximately 30%. These experiments suggest that I_{Na} is involved in the invasion process, probably through its participation to the regulation of the intracellular sodium homeostasis.
© 2003 Elsevier B.V. All rights reserved.

The precise role of ion channels in carcinogenesis and tumour progression is poorly understood. The role of ionic channels in breast cancer cell lines has been focused on potassium channels [1–4]. The role of these channels in cell proliferation was studied mainly in the MCF-7 cell line which is the most extensively studied cell line [1–4]. To the best of our knowledge, in a more metastatic cell line, MDA-MB-231, no electrophysiological study has ever been undertaken to understand the role of ionic channels in the process of proliferation and invasion. The only work we are aware of on a related topic showed that the metastatic properties of this cell line is linked to the absence of a calcium-activated chloride channel, CLCA2 [5].

In this context, the aim of this work is to electrophysiologically characterise MDA-MB-231, MCF-7 and MDA-MB-468 cells. We compared these cell lines because they are usually placed in opposition with regard to their expression or not of oestrogen receptors, the MCF-7 cell line expressing them (therefore called oestrogen receptor-positive, ER^+) while the MDA-MB-231 and MDA-MB-468 do not (therefore called oestrogen receptor-negative,

ER^-). More important to us were their different invasive properties.

The breast cancer cell lines MCF-7, MDA-MB-468 and MDA-MB-231 were purchased from the American Type Culture Collection (Rockville, MD, USA) at passage 151, 340 and 28, respectively. All experiments were carried out within 20 additional passages. Cells were grown in DMEM (4.5 g/l glucose, 584 mg/l glutamine and 3.7 g/l $NaHCO_3$) supplemented at 5% with foetal bovine serum (FBS) and 1% with a mixture of penicillin (5000 U/ml)/streptomycin (5000 μg/ml). Cells were grown in an atmosphere saturated with humidity at 37 °C and 5% CO_2.

For electrophysiological analyses, cells were seeded into 35-mm Petri dishes at 2500 cells/cm^2. Before patch-clamping, the growth medium was rinsed and replaced with a physiological saline solution (PSS, see latter for the ionic composition). Patch pipettes were pulled from non-heparinised haematocrit tubes to a resistance of 3–5 MΩ. Currents were recorded under voltage-clamp mode at room temperature using an Axopatch 200 B patch clamp amplifier (Axon Instrument, Burlingame, CA, USA). Analogue signals were filtered at 5 kHz, using a five-pole lowpass Bessel filter, and sampled at 10 kHz using a 1322A Digidata converter. PClamp software (v8.1, Axon Instrument) was used for generation of voltage commands, acquisition and analysis of whole-cell currents. Cells were studied in the ruptured

* Corresponding author. Tel.: +33-2-4736-6130; fax: +33-2-4736-6226.
E-mail address: LeGuennec@Univ-Tours.Fr (J.-Y. Le Guennec).

patch configuration. The patch membrane under the pipette was broken in order to electrically access the interior of the cell and dialyze it with the intrapipette solution (see below). Cell capacitance and series resistance were electronically compensated by about 60%. The P/2 subpulse correction of cell leakage and capacitance was used. The cell under investigation was continuously superfused with PSS or test solutions. The superfusion was performed by positioning the cell under study at the tip of a conical microcapillary that received the outlet of six microcapillaries connected to 20-ml syringes. Inward currents were recorded by depolarising the cells from a holding potential of -100 mV to a maximal test pulse of -5 mV (corresponding to the maximal inward current) for 30 ms every 500 ms. The protocol used to build the current–voltage (I–V) curve was as follows: from a holding potential of -100 mV, the membrane was stepped to potentials between -80 and $+55$ mV, with 5-mV increments, for 50 ms at a frequency of 2 Hz. Availability curves were obtained by applying 50 ms prepulses using the I–V curve procedure followed by a depolarising pulse to -5 mV for 50 ms. In this case, currents were normalised to the amplitude of the test current without a prepulse (i.e., from -100 mV).

Conductance (g) through Na^+ channels was calculated by dividing the peak Na^+ current by the driving force ($E_m - E_{Na}$) where E_{Na} is the equilibrium potential for Na^+ derived from the Nernst equation and E_m the applied voltage normalised to the maximal conductance. Above the maximal conductance, the normalised conductance was set to 1 for clarity. Relative conductance and availability data were fitted with a Boltzmann function of the form:

$$Y = \frac{1}{1 + \exp(V_{1/2} - V^k)} \qquad (1)$$

where Y is the fitted parameter (conductance or availability), $V_{1/2}$ is the voltage at which half-maximal conductance or availability occurs, k is the slope factor determining how steeply conductance or availability change with voltage and V is the command voltage. Current amplitudes were normalised on cells capacitance to take into account differences in cell sizes and expressed as current density (pA/pF).

The PSS had the following composition (in mM): NaCl 140, KCl 4, $MgCl_2$ 1, $CaCl_2$ 2, D-glucose 11.1, and HEPES 10, adjusted to pH 7.4 with 1 M NaOH. N-methyl-D-glucamine (NMDG) and $MgCl_2$ were substituted for sodium to create Na^+-free external solution and calcium to create Ca^{2+}-free external solution, respectively. The intrapipette solution had the following composition (in mM): K-aspartate 110, KCl 10, NaCl 10, $MgCl_2$ 8, K_2-ATP 8, EGTA 10, HEPES 10, adjusted to pH 7.2 with 1 M KOH. Tetrodotoxin (TTX) was added to the PSS at the concentrations indicated in the figure legends. All drugs and chemicals were purchased from Sigma-Aldrich (St. Quentin, France).

The percentage of blocking or reduction of Na^+ current (I_{Na}) was calculated from the difference in peak current generated by a depolarisation to -5 mV with and without the drug. The drug dose–response curves were fitted to a sigmoidal logistic function of the following form:

$$Y = \frac{100}{1 + \left(\dfrac{IC_{50}}{[Drug]}\right)^n} \qquad (2)$$

where Y is the percentage of blocking at a given concentration of drug [Drug], IC_{50} is the concentration of drug at which 50% of the current was blocked; and n is the slope giving the Hill coefficient.

For proliferation assessment, cells were seeded at 4×10^4 cells per well in 12 wells of a 24-well plate for a given condition on two separate experiments. Cells were grown for a total of 5 days, with every other day change of the medium and the different substances tested. Growth and viability of cells were measured as a whole by the tetrazolium salt assay [6].

Migration was analysed in BD Falcon™ 24-well plates receiving 8 µm pore size polyethylene terephtalate membrane BD Biocoat™ cell culture inserts (Becton Dickinson, France). The upper compartment was seeded with 4×10^4 viable cells in DMEM with 5% FBS. The lower compartment was filled with DMEM supplemented with 10% FBS as a chemoattractant. After 24 h at 37 °C, the remaining cells were removed from the upper side of the membrane with a cotton swab, and cells that had migrated and were attached to the lower side were stained with haematoxylin for 2 min and counted in five different random fields using a light microscope at $\times 200$ magnification. In vitro invasion was assessed as above but with the membrane covered with a film of Matrigel®. Migration and invasion assays were performed in triplicate in eight separate experiments for MDA-MB-231 cells and three different experiments for MCF-7 and MDA-MB-468 cells. For easier comparison between cell lines, results obtained for proliferation, migration and invasion were normalised: cells measured in wells or inserts, in the different conditions, were added and the ratio of these sums (total number of cells in presence of drug/total number of cells in control experiments) calculated for each day. The means were then calculated on these daily calculated ratios.

Data are given as mean ± standard error of the mean (n = number of experiments). Significance was determined using a one-way ANOVA followed by a Student–Neumann–Keuls test when appropriate. $P < 0.05$ was considered as statistically significant.

The mean membrane potential of the MCF-7 cells was -27.9 ± 1.4 mV (n = 27 cells), for MDA-MB-468 cells it was -30.5 ± 3.0 mV (n = 7 cells) while it was -29.2 ± 1.6 mV (n = 65 cells) in MDA-MB-231 cells. The differences between the membrane potentials of the cell lines are not significant.

When the holding potential was set to -100 mV and the membrane depolarised to -5 mV for 30 ms, a rapid inward current was triggered in MDA-MB-231 cells (Fig. 1A) but
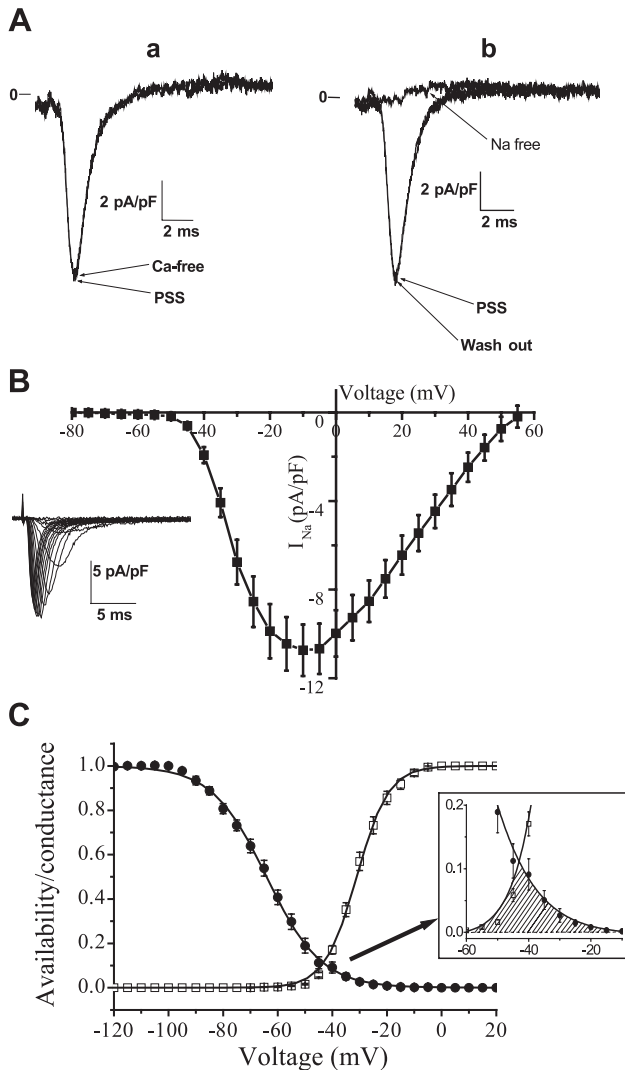
A

B

C

Fig. 1. Ionic and electrophysiological properties of the fast inward current found in MDA-MB-231 cells. (A) Currents, elicited by a 30-ms-long step potential to -5 mV from a holding potential of -100 mV, were recorded (a) with and without 2 mM Ca^{2+}, replaced by Mg^{2+}, in the external medium; (b) with and without 140 mM external Na^+, replaced by NMDG, and after NMDG washout. (B) Mean current–voltage relationship obtained from 26 cells. The inset on the left shows an example of currents recorded from a representative cell depolarised from -50 to $+20$ mV by 5 mV increments. (C) Mean availability–voltage (closed circles) and conductance–voltage (open squares) relationships obtained from 26 cells. Curves are fitted using a Boltzmann function (see text). The half-inactivation voltage and half-conductance voltage are -64.1 ± 0.2 and -31.1 ± 0.1 mV, respectively. The inset on the right magnifies a particular window of voltage in which the current is activated and not fully inactivated and gives place to a window current symbolised by the hatched area.

neither in MCF-7 cells (27 cells studied, data not shown) nor in MDA-MB-468 cells (7 cells studied, data not shown). The inward current was observed in all 65 studied cells but with a density measured varying between 3 and 45 pA/pF with a mean amplitude at -5 mV of -11.4 ± 1.0 pA/pF. Substitution of 2 mM $CaCl_2$ with 2 mM $MgCl_2$ in the PSS surrounding patched cells did not cause any change in the characteristics of the current (Fig. 1A(a)). Conversely,

removal of external sodium ions, substituted with equimolar NMDG, induced the reversible disappearance of the current (Fig. 1A(b)).

To electrophysiologically characterise this sodium current, we constructed I–V curves (Fig. 1B). The threshold of the current takes place approximately -55 mV, the maximum current is obtained at a step potential between -15 and -5 mV and it reverses around $+60$ mV. The availability–voltage curve shown in Fig. 1C indicates that the current starts to inactivate above -100 mV and that inactivation is complete above -10 mV. The superposition of the availability–voltage curve with the conductance–voltage curve on the same graph shows that there is a window of voltage between -60 and -10 mV in which the current is slightly activated and not fully inactivated. Since the membrane potential of these cells is around -30
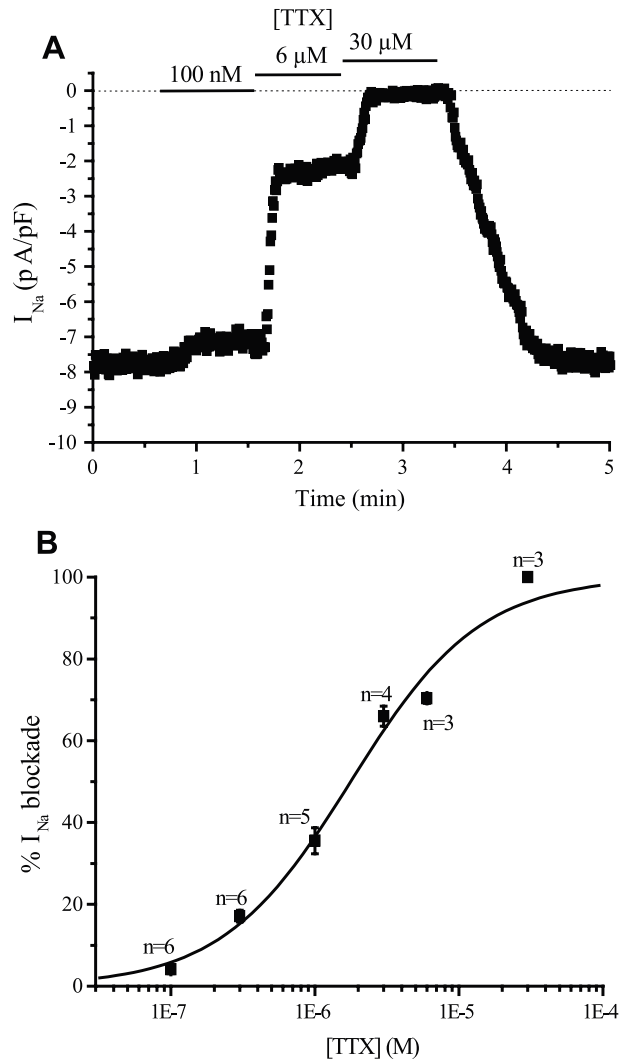
A

B

Fig. 2. Sensitivity of I_{Na} to TTX. (A) Representative effects of different TTX concentrations on the amplitude of I_{Na}. TTX was applied externally to the cell at the time and concentrations indicated on top. (B) Dose–response curve of TTX. Numbers above each point give the number of cells assessed at the given TTX concentration. The logistic fit gives an IC_{50} of 1.78 ± 0.22 μM and a Hill coefficient of 0.97 ± 0.11.

mV, therefore in the voltage window, there must be a continuous entry of sodium ions into the cells through the non-inactivated channels.

Since the fast inward current is a sodium current, we checked its sensitivity to TTX which is the reference blocker of such a conductance [7]. Fig. 2 shows that this current is dose-dependently and reversibly blocked by TTX.

To evaluate the possible role of I_{Na} on oncogenic properties of MDA-MD-231 cells, we first compared the capacity of the three different cell lines to move across a 8-µm pore filter coated (invasion) or not (migration) with Matrigel®. As shown in Fig. 3A and B, MDA-MB-231 cells migrate and invade more than the two other cell lines while MCF-7 is the most "static" cell line. In order to more accurately evaluate the capacity of cells to invade the Matrigel®, we defined a

Matrigel invasion parameter as being the ratio of the mean number of cells in the invasion assay to those in the migration assay (Fig. 3C). MCF-7 is clearly the cell line which has the lowest capacity to invade Matrigel®, while MDA-MB-231 and MDA-MB-468 cells have a similar ability to do it. We then compared these properties without or with 30 µM TTX to fully block the sodium current. Data were normalised for easier comparison between cells lines. As shown on Fig. 3D, cell proliferation for 5 days was not sensitive to the presence of 30 µM TTX in the culture medium in all tested cell lines. In the same way, in the three cell lines, the relative number of cells moving through a membrane of 8-µm pore size was not affected by the presence of TTX in the upper chamber (Fig. 3E). Interestingly, the presence of Matrigel® on the upper part of the
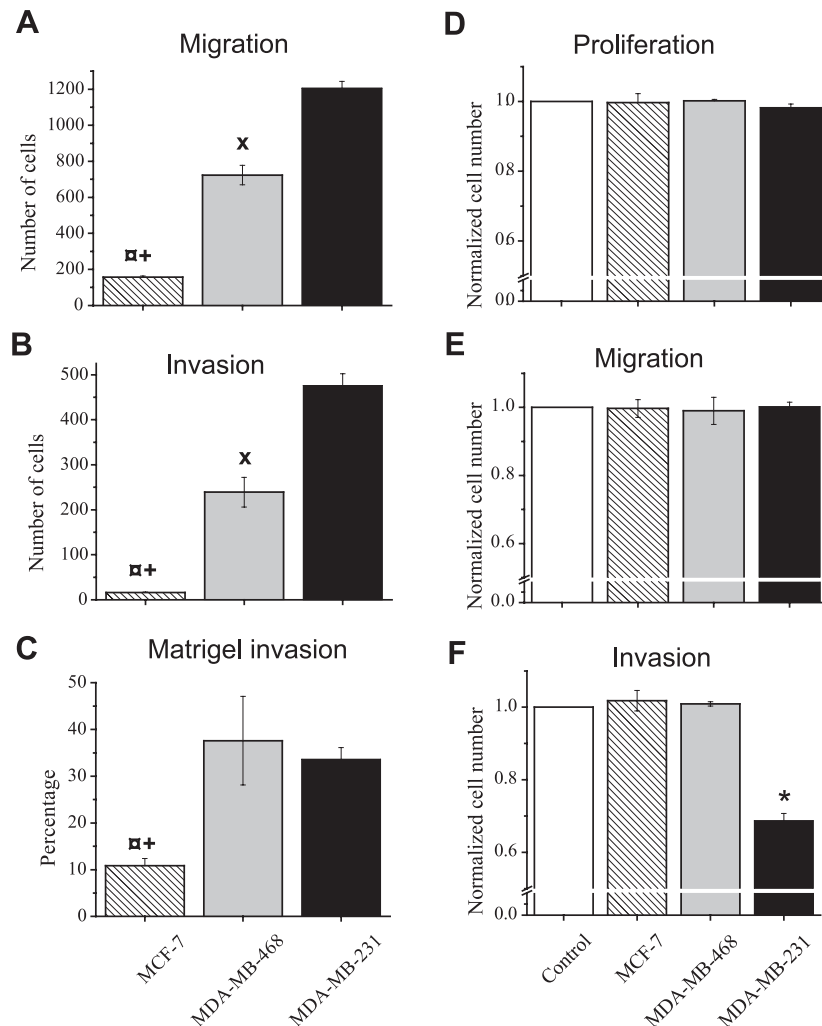

Fig. 3. Comparison of migration, invasiveness and Matrigel invasion of three breast cancer cell lines: MDA-MB-231, MCF-7 and MDA-MB-468 without and with TTX. (A) Migration and (B) invasion show the mean of the total number of cells observed in five different fields per insert. (C) Matrigel invasion is defined as the ratio of the mean number of cells which migrated through a membrane coated with Matrigel® to the mean number of cells which migrated through a non-coated membrane. Matrigel invasion ratios were calculated only when migration and invasion experiments were performed on the same days. (D, E, and F) Relative effects of 30 µM TTX on proliferation and survival (D, proliferation), motility (E, migration) and invasiveness (F, invasion) as compared to control. Results are normalised as explained in the text. Statistically different at $P < 0.05$ when comparing: *, TTX vs. control conditions; ¤, MCF-7 vs. MDA-MB-468 cells; +, MCF-7 vs. MDA-MB-231 cells; ×, MDA-MB-468 vs. MDA-MB-231 cells.

membrane revealed an effect of TTX on the invasion of MDA-MB-231 cells through the membrane (Fig. 3F) without any effect on MCF-7 and MDA-MB-468 cells. Thus, it is clear that proliferation and migration were not sensitive to TTX while invasion was, in MDA-MB-231 cells only.

The role of ionic channels, mainly potassium channels, has been extensively studied in cell proliferation. However, the possible involvement of such proteins in other oncogenic properties has never been described in breast cancer cell lines. To our knowledge, this is the first time that such a fast inward sodium current has been described in a human breast cancer cell line. Interestingly, a voltage-activated, TTX-sensitive, sodium current has been found in metastatic rat and human prostate cell lines. This current, which is lacking in poorly metastatic cell lines, is involved in the invasion but not in the proliferation process [8,9]. Up to now, nine isoforms of the main (alpha) subunit of the channel have been described [7]. Na^+ channels expressed in prostatic and breast cancer cells are likely to differ in their alpha subunits. Indeed, the sodium channel expressed in strongly metastatic prostatic cell lines is the neuronal isoform (designated $Na_V1.7$) which is sensitive to TTX at the nanomolar range [10]. In MDA-MB-231 cells, the current is roughly 100 times less sensitive to TTX than in metastatic prostatic cells. Thus, this current would be classified as a TTX-resistant current [7]. According to its pharmacology, we can exclude the neuronal and the skeletal isoforms which display a TTX sensitivity at the nanomolar range. The best candidate appears to be the cardiac isoform, $Na_V1.5$. In MDA-MB-231, this isoform presents almost the same TTX IC_{50}, has similar kinetics of activation and inactivation but its current–voltage curve displays a rightward shift of 15–20 mV, in comparison to the one found in cardiac cells.

It is interesting to note that intracellular sodium homeostasis has been reported to be important in the development of cancer [11]. These investigators reported that epithelial cancer cells had an intracellular sodium concentration higher than normal epithelial cells. This increase in intracellular sodium might be, at least partially, linked to the activity of such a conductance. Indeed, the voltage dependence of the current clearly indicates that the mean membrane potential of MDA-MB-231 cells allows for a window current responsible for a small influx of sodium into the cell which might participate to an increased intracellular sodium concentration. How the activity of this sodium channel participate to the invasiveness is yet to be determined. We can postulate that the invasiveness of these cells is under the control of proteolytic enzymes such as matrix metalloproteases (MMPs) [12]. It is thus possible that I_{Na}, through a possible regulation of the intracellular sodium homeostasis, regulates the expression, secretion or the activity of MMPs.

In conclusion, we describe for the first time the presence of a fast inward sodium current in an invasive cell line, MDA-MB-231. This current is missing in the weakly invasive cell lines, MCF-7 and MDA-MB-468. The blockade of this current by a specific blocker, TTX, reduced the invasive capacity of MDA-MB-231 cells while TTX had no effect in the other cell lines in which this current was not found. These results raise the possibility that I_{Na} might contribute to the invasive behaviour of some breast cancer cell lines (and thus metastatic behaviour?), but I_{Na} is not a characteristic feature since it is lacking in MDA-MB-468 cells. We hypothesise that among other phenomena involved in invasion, this current might participate in the digestion of the extracellular matrix through the regulation of intracellular sodium homeostasis.

References

[1] W. Wonderlin, K. Woodfork, J. Strobl, Changes in membrane potential during the progression of MCF-7 human mammary tumour cells through the cell cycle, J. Cell. Physiol. 165 (1995) 177–185.

[2] K. Woodfork, W. Wonderlin, V. Peterson, J. Strobl, Inhibition of ATP-sensitive potassium channels causes reversible cell-cycle arrest of human breast cancer cells in tissue culture, J. Cell. Physiol. 162 (1995) 163–171.

[3] H. Ouadid-Ahidouch, F. Chaussade, M. Roudbaraki, C. Slomianny, E. Dewailly, P. Delcourt, N. Prevarskaya, Kv1.1 K^+ channels identification in human breast carcinoma cells: involvement in cell proliferation, Biochem. Biophys. Res. Commun. 278 (2000) 272–277.

[4] H. Ouadid-Ahidouch, X. Le Bourhis, M. Roudbaraki, R. Toillon, P. Delcourt, N. Prevarskaya, Changes in the K^+ current–density of MCF-7 cell during progression through the cell cycle: possible involvement of a h-ether.a-gogo K^+ channel, Recept. Channels 7 (2001) 345–356.

[5] A. Gruber, B. Pauli, Tumorineginity of human breast cancer is associated with loss of the Ca^{2+}-activated chloride channel CLCA2, Cancer Res. 59 (1999) 5488–5491.

[6] T. Mosmann, Rapid colorimetric assay for cellular growth and survival: application to proliferation and cytotoxicity assays, J. Immunol. Methods 65 (1983) 55–63.

[7] A.L. Goldin, Resurgence of sodium channel research, Annu. Rev. Physiol. 63 (2001) 871–894.

[8] P. Smith, N. Rhodes, A. Shortland, S. Fraser, M. Djamgoz, Y. Ke, C. Foster, Sodium channel protein expression enhances the invasiveness of rat and human prostate cancer cells, FEBS Lett. 423 (1998) 19–24.

[9] S. Fraser, J. Grimes, M. Djamgoz, Effects of voltage-gated ion channel modulators on rat prostatic cancer cell proliferation: comparison of strongly and weakly metastatic cell lines, Prostate 44 (2000) 61–76.

[10] J.K. Diss, S. Archer, J. Hirano, S.P. Fraser, M. Djamgoz, Expression profiles of voltage-gated Na^+ channel α-subunit genes in rat and human prostate cancer cell lines, Prostate 48 (2001) 165–178.

[11] I. Cameron, N. Smith, T. Pool, R. Sparks, Intracellular concentration of sodium and other elements as related to mitogenesis and oncogenesis in vivo, Cancer Res. 40 (1980) 1493–1500.

[12] M. Egeblad, Z. Werb, New functions for the matrix metalloproteinases in cancer progression, Nat. Rev. Cancer 2 (2002) 161–174.